Werk

Jahr: 1984
Kollektion: fid.geo
Signatur: 8 Z NAT 2148:54
Digitalisiert: Niedersächsische Staats- und Universitätsbibliothek Göttingen
Werk Id: PPN1015067948_0054
PURL: http://resolver.sub.uni-goettingen.de/purl?PPN1015067948_0054

LOG Id: LOG_0039
LOG Titel: Reduction of satellite magnetic anomaly data
LOG Typ: article

Übergeordnetes Werk

Werk Id: PPN1015067948
PURL: http://resolver.sub.uni-goettingen.de/purl?PPN1015067948
OPAC: http://opac.sub.uni-goettingen.de/DB=1/PPN?PPN=1015067948

Contact

Niedersächsische Staats- und Universitätsbibliothek Göttingen
Georg-August-Universität Göttingen
Platz der Göttinger Sieben 1
37073 Göttingen
Germany
Email: gdz@sub.uni-goettingen.de

J Geophys (1984) 54:207–212

Journal of Geophysics

Reduction of satellite magnetic anomaly data

R.A. Langel [1] *, **E.V. Slud** [2], **and P.J. Smith** [2]

[1] Bullard Laboratories, University of Cambridge, Cambridge CB3 OEZ
[2] Department of Mathematics, University of Maryland, College Park, Md. 20742, USA

Abstract. Analysis of global magnetic anomaly maps derived from satellite data is facilitated by inversion to the equivalent magnetization in a constant thickness magnetic crust or, equivalently, by reduction to the pole. Previous inversions have proven unstable near the geomagnetic equator. The instability results from magnetic moment distributions which are admissible in the inversion solution but which make only small contribution to the computed values of anomaly field. Their admissibility in the solution could result from noisy or incomplete data or from small poorly resolved anomalies. The resulting magnetic moments are unrealistically large and oscillatory. Application of the method of principal components (e.g. eigenvalue decomposition and selective elimination of less significant eigenvectors) is proposed as a way of overcoming the instability and the method is demonstrated by applying it to the region around the Bangui anomaly in Central Africa.

Key words: Satellite magnetic anomalies – Crustal anomalies – Crustal magnetization – Equivalent source

Introduction

Dampney (1969) described a method for synthesizing bouguer gravity measurements on an irregular (3 D) grid. The synthesis consisted of a mathematical representation of the data in terms of discrete point masses at some, arbitrary, fixed depth below the earth's surface. Mayhew (1979) adapted this method to the synthesis of magnetic anomaly data acquired by the POGO satellites. In this method the satellite magnetic anomaly data is represented by an array of dipoles at the earth's surface. The dipoles are assumed to be aligned along the direction of the earth's main field, as determined by a spherical harmonic model, and their magnitudes are determined so as to best reproduce the anomaly data in a least-squares sense. Following Dampney (1969) this is called an equivalent source model. The resulting dipole moments can be converted to depth-integrated magnetization, provided the appropriate depth is known. Initially, Mayhew (1979) used a dipole spacing of 4° in latitude and longitude to model the United States region. He then used the calculated anomaly field from this equivalent source model as smoothed input to a second model in which the sources were 2° by 2° spherical prisms 40 km thick. Furthermore, the magnetic moments of the prisms were constrained to be specified by the coefficients in a double Fourier series in latitude and longitude. Use of the Fourier constraint was intended to minimize instability in the magnetization solution. Mayhew attributed instability to the "amplification" of high frequencies in the data. High frequencies are particularly common near the auroral belts where data may be "contaminated" by the presence of fields from ionospheric currents.

In a later publication, Mayhew et al. (1980) abandoned the Fourier constraint and derived equivalent magnetization directly from the initial dipole moment solution. Data over Australia were analyzed in two parts, east and west, and the results combined. As part of their analysis, the authors examined the question of the stability of the dipole solution as a function of dipole spacing in degrees. Figure 1

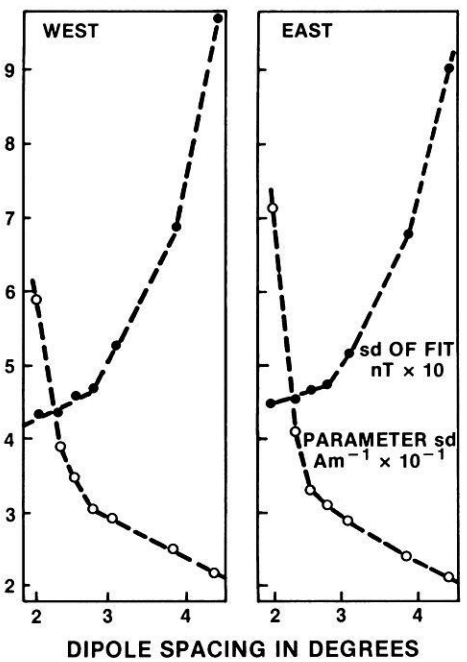

Fig. 1. Trade-off between standard deviation of fit of equivalent source magnetic anomaly field and observed field vs. "stability" of inversion as indicated by standard deviation of magnetization solution parameters. Optimal dipole spacing is taken to be about 2.7°. From Mayhew (1980)

* On sabbatical from the Geophysics Branch, Goddard Space Flight Center, Greenbelt, Maryland 20771, USA

Offprint requests to: R.A. Langel

(Fig. 3 from Mayhew et al., 1980) is a plot of the standard deviation, sd, as a function of dipole spacing. (Also shown is the standard deviation of the fit.) The parameter sd is seen to increase slowly as the dipole spacing is reduced until, at about 2.7°, it begins to increase rapidly as the dipole spacing is further reduced. Also, at this point plots of the dipole moments begin to exhibit an oscillatory instability in which, in its extreme, adjacent sources take on alternately large positive and negative values. Contours of the magnetic moments exhibit a bulls-eye pattern with, obviously, no physical meaning. The authors conclude that 2.7° is the optimal dipole spacing. Magnetization values (defined as magnetic moment per unit volume) are determined under the assumption that the magnetic crust is 40 km thick with constant magnetic moment throughout this layer. Because the satellite altitude is large compared to 40 km, the anomalies computed from the equivalent source solution depend directly upon the product of magnetization and layer thickness, i.e. if the magnetization is doubled and the thickness halved the computed anomaly will be unchanged. Working independently, von Frese et al. (1981) proposed the same method of analysis, only applied to gravity as well as magnetic anomaly data.

In a re-analysis of the data from the U.S. region, Mayhew (1982) now used equal-area spacing of the dipoles. In an analysis similar to that leading to Fig. 1, he found the optimal dipole spacing to be about 300 km, or again near 2.7°. At closer spacing the standard deviation of the dipole parameters increased exponentially and the magnetization solution showed symptoms of instability.

Published results using Mayhew's technique have all been at midlatitudes. When the method is used at or within about 20° of the geomagnetic equator, extreme instability is present for any reasonable dipole spacing. Because our research calls for equivalent magnetization maps of the world (or, equivalently, reduced-to-pole anomaly maps) we have attempted to find a way to derive stable solutions at any latitude and at any dipole spacing.

The method

Let

$$B_i = \sum_{j=1}^{m} a_{ij}\beta_j + \varepsilon_i,\ i = 1, \ldots, n \tag{1}$$

where: B_i is the anomaly field at the i-th satellite position.
β_j is the magnetic moment of the j-th dipole.
m is the number of dipoles in the solution,
a_{ij} is the geometric source function relating the j-th source to the i-th position.
ε_i are the errors due to instrument noise, field sources other than anomalies, etc.

In the least squares procedure we estimate the $\{\beta_j\}$ with $\{b_j\}$ by minimizing

$$R = \sum_{i=1}^{n} \left[B_i - \sum_{j=1}^{m} a_{ij} b_j \right]^2. \tag{2}$$

In matrix notation one must solve

$$A^T A b = A^T B. \tag{3}$$

Instability is due to a high degree of collinearity among the columns of A: certain linear combinations of the columns are nearly zero. This means that for some choice of coefficients, say v_j, $\sum a_{ij} v_j \sim 0$ for all i implying that:

$$\sum a_{ij} b_j \sim \sum a_{ij} b_j + K \sum a_{ij} v_j. \tag{4}$$

Hence substantial perturbations of b_j will have little effect on the fitted field value and, conversely, measured field values exert little constraint on these b_j.

A test for multicollinearity is provided by the condition number of the matrix $A^T A$, defined as the ratio λ_1/λ_m, where λ_1 and λ_m are the largest and smallest eigenvalues of $A^T A$.

In deriving equivalent source solutions at geomagnetic latitudes above about 30°, typical condition numbers are in the 100–600 range. Near the geomagnetic equator, on the other hand, values are typically over 6000.

As a remedy for these shortcomings, the technique of *principal components regression* is proposed. This is a modification of the method of least squares whose effect is to smooth the resulting equivalent source model, while maintaining a high level of agreement between the observed and fitted anomaly field. The elements of principal components regression are set forth below.

One begins with the singular value decomposition (Stewart, 1973) of the matrix A:

$$A = U D V^T \quad \text{or} \quad A V = U D \tag{5}$$

where U is an $n \times n$ matrix whose columns are eigenvectors of $A A^T$, V is an $m \times m$ matrix whose columns are eigenvectors of $A^T A$, and D is an $n \times m$ matrix with non-negative entries, $d_1 \geqq \ldots \geqq d_m \geqq 0$ along the main diagonal and zeros elsewhere. The values d_i^2 are eigenvalues of both $A^T A$ and $A A^T$.

The orthogonal matrices U and V are used to transform the observations and parameters as follows.
One writes:

$$Z = U^T B;\ \gamma = V\beta \text{ and } \delta = U^T \varepsilon, \tag{6}$$

Then the model, (1), becomes:

$$Z = D\gamma + \delta. \tag{7}$$

The quantities in the normal equations are transformed similarly:

$$A^T A\beta = V D^T D\gamma,\ A^T B = V D^T Z, \tag{8}$$

so that the estimates for γ are

$$c_j = D_j^{-1} Z_j \tag{9}$$

with:

$$\text{Var } c_j = d_j^{-2}\sigma^2 \text{ and Cov } (c_j, c_k) = 0. \tag{10}$$

Immediately one observes that when d_j is small, c_j has high variance.

In the original coordinate system one can write

$$\left| \sum_{j=1}^{m} a_{ij} v_{jk} \right| = |u_{ik} d_k| \leqq d_k \tag{11}$$

because U is orthogonal. Therefore small d's correspond to eigenvectors representing souces of multicollinearity. If

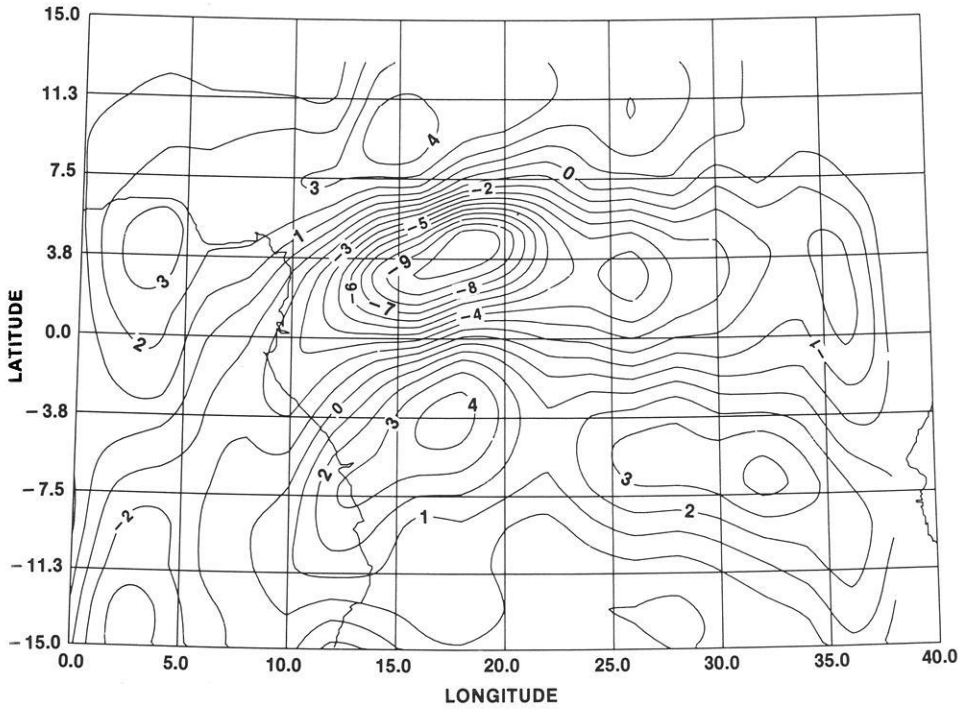

Fig. 2. Average scalar anomaly field from POGO data. Averages are taken in $2° \times 2°$ bins. Contour interval is 1 nT

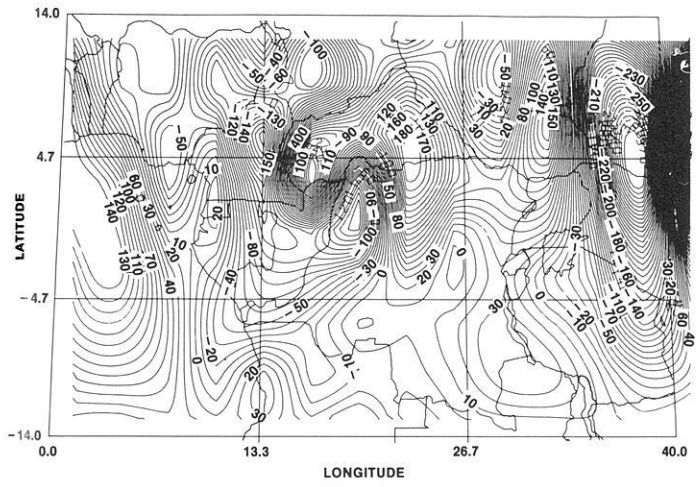

(a) P(%) = 100%

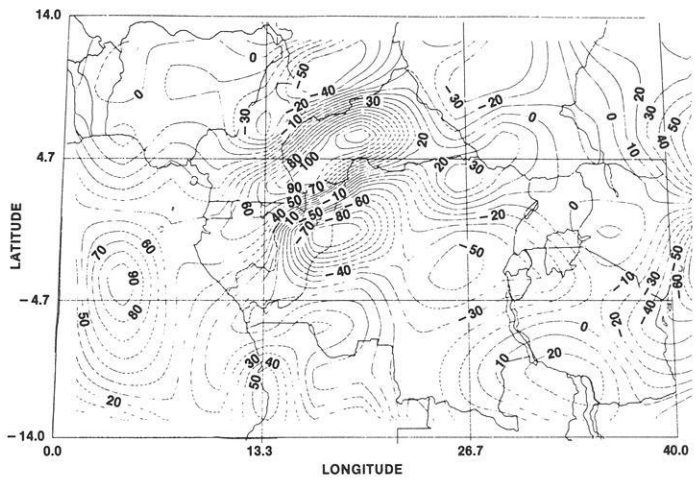

(b) P(%) = 99%

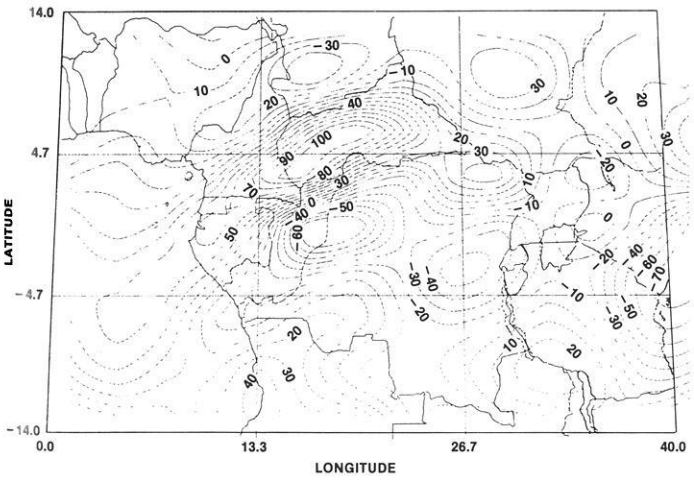

(c) P(%) = 97%

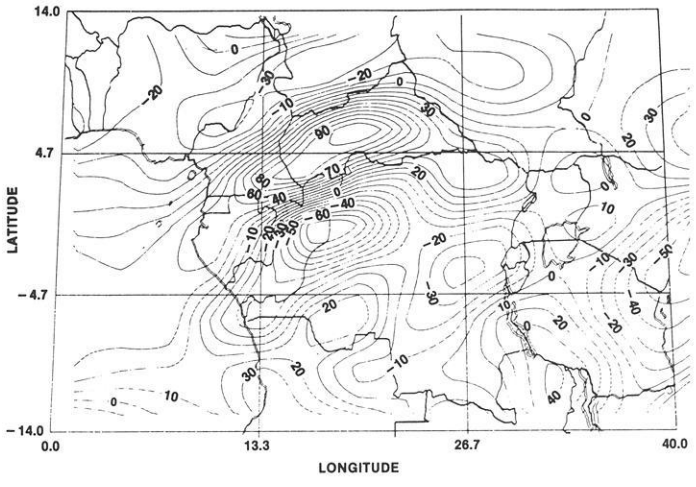

(d) P(%) = 95%

Fig. 3. Magnetization contours from equivalent source solutions. Varying cutoffs in principal components analysis. Units are 0.01 Amp/m. Contour interval is 10

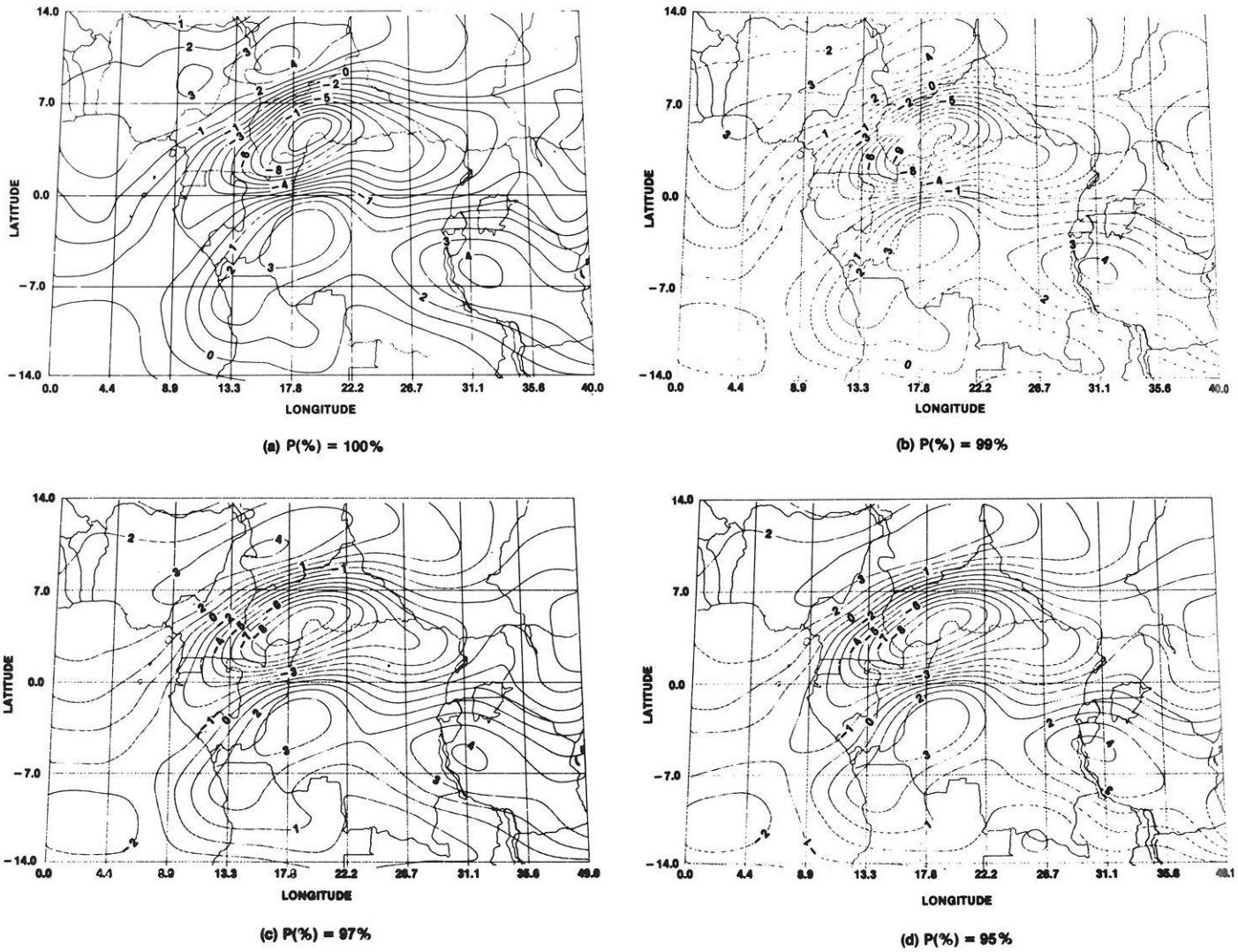

Fig. 4. Anomaly field computed at 500 km altitude from equivalent source solution. Varying cutoffs in principal components analysis. Contour interval is 1 nT

d_k is very small, γ_k is estimated imprecisely. But through the transformations $\beta = V^T\gamma$, $b = V^T c$, this imprecision is propagated throughout the estimated parameter vector b.

Now the rationale for the principal component method can be seen. If d_k is small, the corresponding a_k is noisy, i.e., an imprecise estimate, whose variability makes the stimate b unreliable. Furthermore, the corresponding quantity $\sum_j a_{ij} v_{jk}$ is uniformly small and may safely be replaced by 0. This process is equivalent to replacing c_k by 0. An algorithm is:

(a) Compute $A^T A$ and solve $A^T A b = A^T B$ for b.
(b) Compute the eigenvalues $d_1^2, \ldots, d_m^2$ and V, the corresponding matrix of eigenvectors.
(c) Transform to obtain $c = Vb$.
(d) Define c^* by $c_j^* = c_j$ if $j \leqq k^*$
$= 0$ if $j > k^*$
where $\sum_1^{k^*} d_j^2 / \sum_1^m d_j^2 = P$, where P and k^* are to be determined.
(e) Compute $b^* = V^T c^*$.

The large matrix U is not computed, so the computation is manageable. The determination of k^*, the number of eigenvectors retained, and P, the percent of the trace of D, in step (d) is the crucial decision in applying the method.

Application of the method

Central Africa, in which the Bangui Anomaly (Regan and Marsh, 1982) is situated, was chosen for a test case. Figure 2 shows an anomaly map of the area derived by computing and contouring 2° averages of data from the POGO satellites. These same data were then used to derive an equivalent source solution. Figure 3 shows magnetization contours for four values of P and Fig. 4 shows the corresponding anomaly field computed from the equivalent source solution.

Intercomparison of the computed anomaly fields between Figs. 4a through d shows only small differences between the four solutions. Furthermore, comparison with Fig. 2 shows that the original data is reproduced in a satisfactory fashion. In fact, the representations of Figure 4 are preferable because they are at constant altitude (500 km)

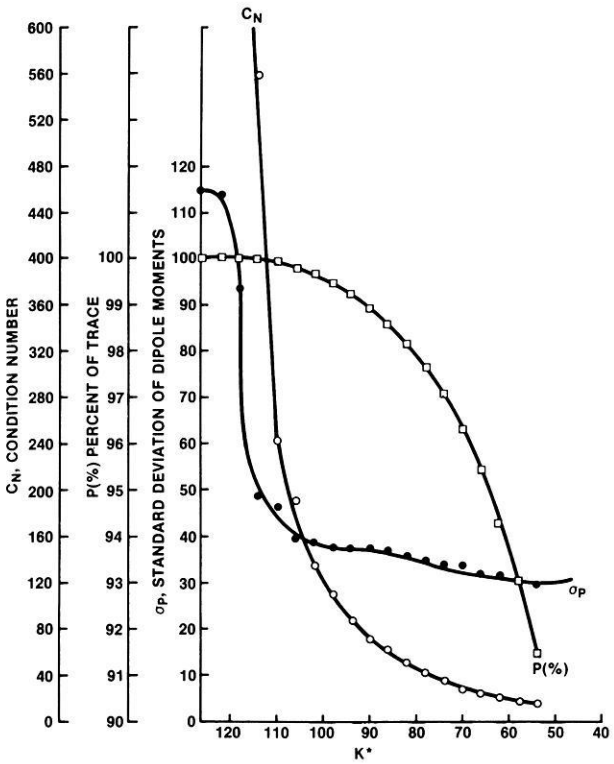

Fig. 5. Variation of solution parameters (Cn, condition number; P, percent of trace; σp, standard deviation of dipole moments) as a function of k^*, the number of retained eigenparameters

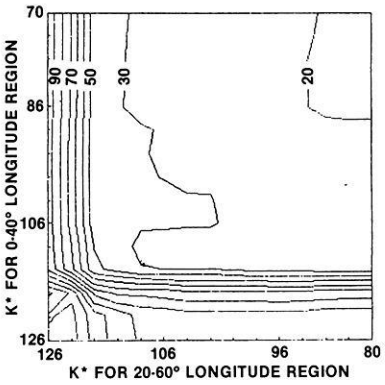

Fig. 6. Rms difference in magnetization (A m^{-1}) in overlap region between the 0–40° longitude and 20–60° longitude solutions where the latitude is $\pm 14°$

and the high frequency noise is smoothed. However the differences in magnetization values between Figs. 3 are dramatic. Figure 3a shows extremely high and variable magnetization values, and high gradients, and the magnetization pattern shows poor correspondence with the anomalies of Fig. 2. In contrast, Fig. 3b, 3c and 3d show more reasonable values of magnetization, lower gradients, and magnetization patterns with definite correspondence to the original anomaly data. Figure 3d is noticeably "smoother" than Fig. 3b and 3c and, in this case, the principal components analysis can be viewed as a form of low pass filter.

The question is, can we find an objective method for choosing a value of P which gives a magnetization result which has some physical credence? Figure 5 shows plots of P (%), condition number (Cn), and parameter sd (after Mayhew et al., 1980, and Mayhew, 1982) as a function of k^*. Such a plot certainly gives helpful guidelines. It shows that a large number of eigenparameters can be discarded before any significant change in P occurs. For example, the full set of parameters is 126. For $k^*=94$ P is only reduced to 99% while large improvements are evident in condition number and sd. Typical values of sd at higher latitudes, where the instability has only small effect, are between 30 and 40. We might then expect that k^* should be chosen so that sd is in that range. In the present case this gives k^* from 60 to 106, P from 93.5% to 99.7%, and condition number from 20 to 189.5. Unfortunately, none of the curves on Fig. 5 show a sharp break or any other indication, in this k^* range, to help us pin down a value of k^* more closely.

In practice, maps of magnetization are generally derived by piecing together solutions from adjacent areas. Area size is determined by computer limitations. Because we are dealing with finite areas and data sets, each solution has a certain amount of "edge effect", i.e. the magnetization values are more accurate or realistic in the interior of the solution region. Our practice is to overlap adjacent regions by up to 50%. That is, the solution just to the east of the region of Fig. 2–4 covers the same latitude range and its longitude range is 20–60°. The solution would then be combined along the 30° longitude line. If the two solutions have no edge effect, they will match perfectly where they are joined. In practice there are differences in solutions which manifest themselves as "kinks" along the line where they are joined.

Our final selection of k^* is made by trying to minimize the disjointedness of adjacent solutions. The parameter used is the rms difference of magnetization in the region of overlap. Figure 6 shows a contour plot of this difference as a function of k* for the region of Fig. 2–4 and of k^* for the region adjacent on the east. For high latitude regions, acceptable discontinuties over boundaries are obtained for the rms lower than about 25. It we choose a value of 20 for "safety" we should then pick $k^*<87$ for the 0–40° longitude region and $k^*<90$ for the 20–60% longitude region. Each region has four such sets of constraints, one each for the north, south, east and west boundaries. For the case at hand we chose $k^*=74$ for the 0–40° longitude region and $k^*=86$ for the 20–60° longitude region.

To illustrate the results of combining general solutions, Figure 7 shows a composite of four solutions. The solutions are joined along the longitude = 30° line and the latitude = 6° line. Examination of the plot shows evidence of a slight discontinuity at the 30° meridian and of enhanced gradients near the 6° latitude line. Comparison with Fig. 3c also shows some disagreement between the extreme boundaries of Fig. 3c and the alternate solution used to derive Fig. 7. Edge effects like this seem unavoidable. [Note, the discontinuties along latitude = 0° are artifacts of the contouring software.]

Figure 7 represents what we regard to be a reasonable estimate of equivalent crustal magnetization, relatively free from noise and edge effects, and suitable for interpretation. Any use of such maps should, of course, take into account the uncertainties in its derivation. Such uncertainties are obviously greater for the shorter wavelength features. To our mind, such maps are to be regarded as reconnaissance tools for large scale correlations with other geologic and geophysical data and for the initial step in the forward

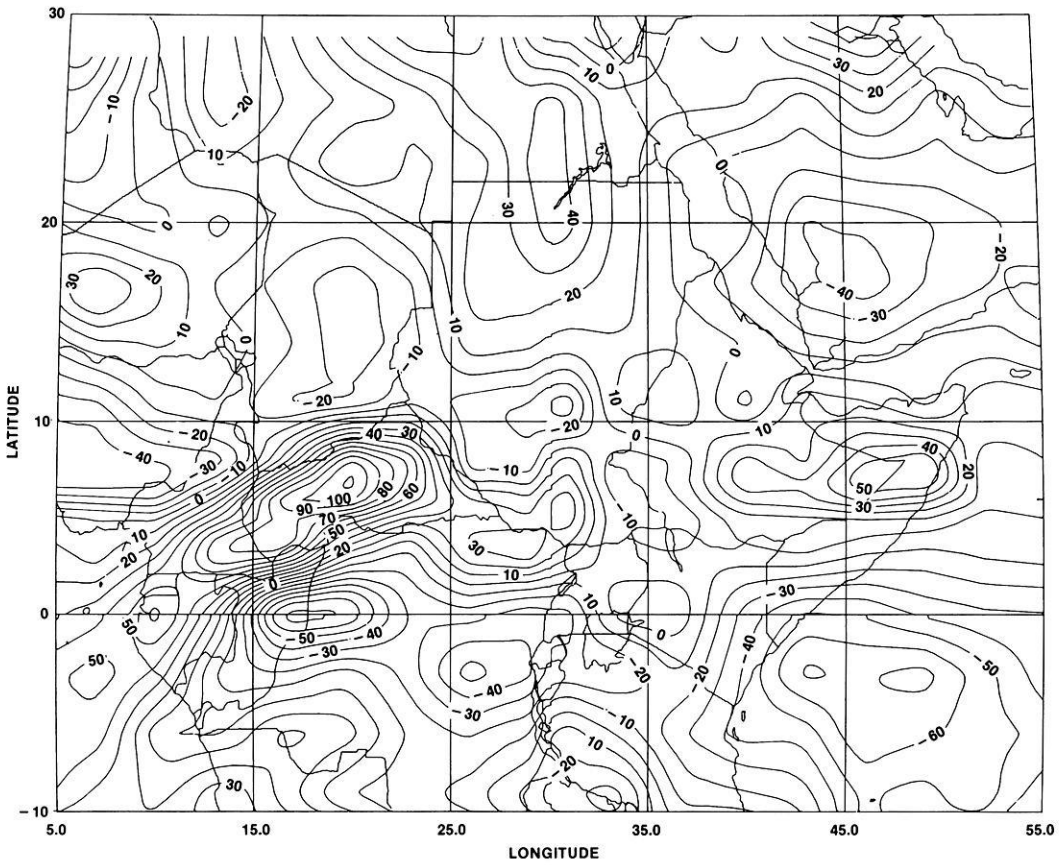

Fig. 7. Magnetization contours from combined equivalent source solutions. Units are 0.01 Amps/m. Contour interval is 10. Four solutions are joined along 6° latitude and 30° lingitude

modeling of specific anomalies needed for detailed interpretation.

Acknowledgments. We are indebted to F. Gertler, S.D. Oh, R. Horner, J. Richardson and J. Rice for implementing this analysis on the computer. E.V.S. and P.J.S. were supported by NASA contract NGL 21-002-033.

References

Dampney, C.N.G.: The equivalent source technique: Geophysics **45**, 39–53, 1969

Mayhew, M.A.: Inversion of satellite magnetic anomaly data: J. Geophys. **45**, 119–128, 1979

Mayhew, M.A.: An equivalent layer magnetization model for the United States derived from satellite altitude magnetic anomalies: J. Geophys. Res. **87**, 4837–4845, 1982

Mayhew, M.A., Johnson, B.D., Langel, R.A.: An equivalent source model of the satellite-altitude magnetic anomaly field over Australia: Earth Planet. Sci. Lett. **51**, 189–198, 1980

Regan, R.D., Marsh, B.D.: The Bangui magnetic anomaly: its geological origin: J. Geophys. Res. **87**, 1107–1120, 1982

Stewart, G.W.: Introduction to Matrix Computations. New York: Academic Press 1973

von Frese, R.R.B., Hinze, W.J., Braile, L.W.: Spherical earth gravity and magnetic anomaly analysis by equivalent point source inversion: Earth Planet. Sci. Lett. **53**, 69–83, 1981

Received August 17, 1983; Revised November 25, 1983
Accepted November 28, 1983